The current issue and full text archive of this journal is available at
www.emeraldinsight.com/0961-5539.htm

Parametric analysis of entropy generation due to laminar developing mixed convection between differentially heated isothermal vertical parallel plates

Esmail M.A. Mokheimer
Mechanical Engineering, King Fahd University of Petroleum & Minerals (KFUPM), Dhahran, Saudi Arabia

Received 23 April 2009
Reviewed 21 June 2009
Revised 10 September 2009, 23 October 2009
Accepted 18 November 2009

Abstract

Purpose – The aim of this article is to present the results of a parametric analysis of the entropy generation due to mixed convection in the entry-developing region between two differentially heated isothermal vertical plates.

Design/methodology/approach – The entropy generation was estimated via a numerical solution of the mass, momentum and energy conservation equations governing the flow and heat transfer in the vertical channel between the two parallel plates. The resultant temperature and velocity profiles were used to estimate the entropy generation and other heat transfer parameters over a wide range of the operating parameters. The investigated parameters include the buoyancy parameter (*Gr*/*Re*), Eckert number (*Ec*), Reynolds number (Re), Prandtl number (Pr) and the ratio of the dimensionless temperature of the two plates (θ_T).

Findings – The optimum values of the buoyancy parameter (*Gr*/*Re*) optimum at which the entropy generation assumes its minimum for the problem under consideration have been obtained numerically and presented over a wide range of the other operating parameters. The effect of the other operating parameters on the entropy generation is presented and discussed as well.

Research limitations/implications – The results of this investigation are limited to the geometry of vertical channel parallel plates under isothermal boundary conditions. However, the concept of minimization of entropy generation via controlling the buoyancy parameter is applicable for any other geometry under any other thermal boundary conditions.

Practical implications – The results presented in this paper can be used for optimum designs of heat transfer equipment based on the principle of entropy generation minimization with particular focus on the optimum design of plate and frame heat exchanger and the optimization of electronic packages and stacked packaging of laminar-convection-cooled printed circuits.

Originality/value – This paper introduces the entropy generation minimization via controlling the operating parameters and clearly identifies the optimum buoyancy parameter (*Gr*/*Re*) at which entropy generation assumes its minimum under different operating conditions.

Keywords Convection, Plate structures, Flow, Numerical analysis
Paper type Research paper

Nomenclature

b	gap width between the parallel plates and the characteristic length of current problem	dp/dz	pressure gradient
		dP/dZ	dimensionless pressure gradient
		Ec	Eckert number, $u_0^2/C_p(T_1 - T_0)$
C_p	specific heat of fluid at constant pressure	Gr	Grashof number, $g\beta(T_1 - T_o)b^3/\nu^2$

The author would like to express his sincere acknowledgment to KFUPM for the support of this work through project No. SB080006.

International Journal of Numerical Methods for Heat & Fluid Flow
Vol. 20 No. 8, 2010
pp. 941-971

0961-5539
DOI 10.1108/09615531011081450

Gr/Re	modified buoyancy parameter
$(Gr/Re)_{optimum}$	optimum value of the modified buoyancy parameter
g	gravitational body force per unit mass (acceleration)
h	convective heat transfer coefficient
l	channel height
p	local pressure at any cross-section of the vertical channel
p_o	hydrostatic pressure, $\rho_0 gz$ at channel entrance
P	dimensionless pressure inside the channel at any cross-section, $(p - p_o)/\rho_o u_o^2$
Pr	Prandtl number, $\mu C_p/k$
Re	Reynolds number, $\rho_o u_o b/\mu$
s'''_{gen}	total volumetric entropy generation rate
$s'''_{Thermal}$	volumetric thermal entropy generation rate
s'''_{Visous}	volumetric viscous entropy generation rate
s_{Tot}	total entropy generation rate
S_{gen}	dimensionless volumetric entropy generation rate, $s'''_{gen} b^2/k$
$S_{Thermal}$	dimensionless volumetric thermal entropy generation rate
$S_{Viscous}$	dimensionless volumetric viscous entropy generation rate
S_{TotY}	dimensionless total entropy generation rate across the channel width
$(S_{TotY})_{Tm}$	dimensionless total thermal entropy generation rate across the channel width
$(S_{TotY})_{Vs}$	dimensionless total viscous entropy generation rate across the channel width
S_{Tot}	dimensionless total entropy generation rate
$(S_{Tot})_{Tm}$	dimensionless total thermal entropy generation rate
$(S_{Tot})_{Vs}$	dimensionless total viscous entropy generation rate
T	dimensional temperature at any point in the channel
T_0	ambient (reference) temperature or fluid inlet temperature
T_1, T_2	isothermal temperatures of plate 1 and plate 2 of parallel plates
u	axial velocity component
$\overline{u}$	average axial velocity
u_0	uniform entrance axial velocity
U	dimensionless axial velocity at any point, u/u_o
v	transverse velocity component
V	dimensionless transverse velocity, $v\,Re/u_o$
y	transverse coordinate of the vertical channel between parallel plates
Y	dimensionless transverse coordinate, y/b
z	axial coordinate (measured from the channel entrance)
Z	dimensionless axial coordinate in Cartesian and cylindrical coordinate systems, z/bRe

Greek letters

μ	dynamic viscosity of the fluid
υ	kinematic viscosity of the fluid, μ/ρ_o
θ	dimensionless temperature, $T - T_o/T_1 - T_o$

θ_T wall temperature difference ratio, $(T_2 - T_o)/(T_1 - T_o)$

ρ density of the fluid

ρ_0 density of the fluid at the channel entrance

τ dimensionless extreme temperature, $T_o/(T_1 - T_o)$

1. Introduction

Analysis of flow and heat transfer in channels and parallel-plate ducts have been the focus of many researchers' interest over the last few decades. This configuration is encountered in many of energy-related applications such as solar energy collection, as in the conventional flat plate collector, in the cooling of modern electronic systems and in the plate and frame heat exchangers, which is finding its way in many of the industrial heat transfer equipment and applications. In the electronic equipment and packages, electronic components are mounted on circuit cards, an array of which is positioned vertically in a cabinet forming vertical channels through which coolants are passed (Otani and Tanaka, 1975; EPP staff report, 1981). The coolant may be propelled by forced/mixed convection for large applications. The vertical parallel plate configuration is applicable in the design of electronic equipment cooling systems. The huge amount of the research related to flow and heat transfer through parallel plate channels has been well cited by Peterson and Ortega (1990) in their analysis of thermal control of electronic equipment and the more recent work reported by Du Toit (2000), Spiga and Morini (1996), Schwiebert and Leong (1995), Hao and Chung (1995), Inagaki and Komori (1995).

It is well known that flow and heat transfer processes are always irreversible. In other words, for all heat transfer processes, there exists an entropy generation. This thermodynamic irreversibility, or entropy generation, is attributed to two main sources. One of these sources is the heat transfer due to finite temperature difference, which is referred to as the thermal entropy generation. The other source of irreversibility is attributed to the viscous friction due to fluid flow and is referred to as the viscous entropy generation. The entropy generation of the process, irreversibility, is directly proportional to the amount of dissipated useful energy in the process. Understanding how entropy is being generated, one can reduce the irreversibility of the heat transfer process and consequently enhances its efficiency. An optimal design can be obtained by compromising the pertinent operating parameters in order to minimize the entropy generation. Thermal optimization of a stack of printed circuit boards using entropy generation minimization (EGM) method was recently presented by Yang *et al.* (2008). In this study, Yang *et al.* (2008) numerically integrated the governing thermal-fluid flow equations in the laminar-flow regime subject to the appropriate boundary conditions. After the flow and temperature fields were solved, the volumetric rate of local entropy generation was integrated to determine the total entropy generation rate in the system which consists of two components, one by heat transfer and the other by viscous friction. The Reynolds number, block geometry and bypass flow area ratio were varied to search for an optimal channel spacing. Having the same interest in optimizing stacked packaging of laminar-convection-cooled printed circuits, Takahiro *et al.* (2008) also used the EGM method to optimize the fin pitch of heat sink in a free-convection environment. In connection with the electronic printed circuit packaging and electronic cooling devices, Ilis *et al.* (2008) numerically investigated the effect of aspect ratio on entropy generation in a rectangular cavity with differentially heated vertical walls. The vertical walls of the cavity were at different constant temperatures while the horizontal walls were adiabatic. Heat transfer between vertical walls occurs by laminar natural convection. Based on the obtained dimensionless velocity and temperature values, the

distributions of local entropy generation due to heat transfer and fluid friction, the local Bejan number and local entropy generation number were determined and related maps were plotted for $Pr = 0.7$. On the same area of interest, Zahmatkesh (2008) analyzed the importance of thermal boundary conditions of the heated/cooled walls in heat transfer and entropy generation characteristics inside a porous enclosure, heated from below. On the other hand, Varol *et al.* (2008) studied the entropy generation due to conjugate natural convection heat transfer and fluid flow inside an enclosure which was bounded by two solid massive walls from vertical sides at different thicknesses. Famouri and Hooman (2008) studied effects of the Rayleigh number, the position of the heated partition and the dimensionless temperature difference on the local and average entropy generation rate for natural convection in a partitioned cavity, with adiabatic horizontal and isothermally cooled vertical walls.

Focusing on the entropy generation due to fully developed forced convection in porous-saturated rectangular ducts, Hooman *et al.* (2007) investigated analytically the first and the second law characteristics. In this regard, the Darcy-Brinkman flow model was employed under three different types of thermal boundary conditions. Expressions for the Nusselt number, the Bejan number and the dimensionless entropy generation rate were presented in terms of the system parameters. More recently, Hooman *et al.* (2008a) analytically investigated the entropy generation for thermally developing forced convection in a porous medium bounded by two isothermal parallel plates on the basis of the Darcy flow model where the viscous dissipation effects had also been taken into account. Parallel to this study, Hooman *et al.* (2008b) numerically investigated the entropy generation due to forced convection in a parallel plate channel filled by a saturated porous medium. Two different thermal boundary conditions were considered, being isoflux and isothermal walls. Effects of the Peclet number, the porous medium shape factor, the dimensionless temperature difference for isothermal walls, the dimensionless heat flux for isoflux walls and the Brinkman number on the Bejan number as well as the local and average dimensionless entropy generation rate were examined and reported.

On the other hand, considering the optimization of flow and heat transfer in channels between parallel plates as the basis for optimization of plate and frame heat exchangers, Ordóñez and Bejan (2000), Ko (2006a, b, 2007a, b) and Ko and Cheng (2007) carried out a series of investigations. In this regard, Ordóñez and Bejan (2000) investigated the possibilities of EGM in parallel plates counter flow heat exchangers. The study showed that the entropy generation is directly affected by the spacing ratios between the two channels and the heat transfer area between the two streams which gives the opportunity to minimize the irreversibility by controlling these two factors. Ko (2006a) investigated the effects of longitudinal ribs on laminar forced convection and entropy generation in a curved rectangular duct using numerical methods. The major concern of Ko (2006a) in this article was to explore the optimal rib number and arrangement of the mounted rib based on the minimal entropy generation principle. In a second article, Ko (2006b) reported his analysis of the entropy generation and optimal Reynolds number for developing forced convection in a double sine duct with various wall heat fluxes, which frequently occurs in plate heat exchangers, based on the EGM principle by analytical thermodynamic analysis as well as numerical investigation. Following that, Ko (2007a) numerically investigated the developing laminar forced convection and entropy generation in both double- and half-sine ducts. The optimal analysis of the two-type ducts based on the minimal entropy generation principle was the major concern. Parallel to this, Ko (2007b) investigated the effects of corrugation angle on developing laminar forced convection and entropy generation in a wavy channel with numerical methods.

The effects of corrugation angle on the distributions and magnitudes of local entropy generation resulted from frictional irreversibility and heat transfer irreversibility were discussed in detail. The optimal corrugation angle and favorable Re were reported based on the minimal entropy generation principle. Ko and Cheng (2007) investigated, also numerically, the developing laminar forced convection and entropy generation in a wavy channel. The effects of aspect ratio and Reynolds number (Re) on entropy generation were again their major concerns. The flow features, including secondary flow motion and temperature distribution as well as the detailed distributions of local entropy generation due to frictional and heat transfer irreversibilities were reported. A numerical computation of combined gas radiation and forced convection through two parallel plates was presented by Ben Nejma *et al.* (2008). In their study, they considered a laminar flow of a temperature-dependent and non-gray gas in the entrance region of the channel. Over-heated water vapor was chosen as a gas because of its large absorption bands. They gave some special attention to entropy generation and its dependence on geometrical and thermodynamic parameters.

The literature cited above reveals clearly the importance of the analysis of flow and heat transfer in channels between parallel plates. It also indicates that many researchers have devoted their efforts to the analysis of the flow and heat transfer in such geometry over the last few decades. However, only over the last few years quite a number of researchers focused on the optimization of the flow and heat transfer process in such geometry. Moreover, many of these recent investigations were focused on the natural (free) and forced convection optimization via EGM. However, despite its importance, only few studies investigated the entropy generation due to mixed convections in vertical parallel plate channels. Mixed convection takes place when the forced-convection effects and the free-convection effects are of comparable magnitudes. In mixed-convection flows, the effect of buoyancy force on forced convection becomes significant. This effect is especially pronounced in situations where the forced-flow velocity is low and the temperature difference is large. Mixed-convection flow is called buoyancy-aided flow if the buoyancy forces act in the flow direction while it is called buoyancy-opposed flow if the buoyancy forces oppose the flow direction. In vertical parallel plate configuration, when the spacing between the plates is small relative to the height of the channel, the plates' elevated temperatures and the low Reynolds number establish the mixed convection situations in the channel between the vertical parallel plates. Constant property fully developed and developing mixed convection between vertical parallel plates has been of interest in research for many years (Ostrach, 1954; Lietzke, 1954; Cebeci *et al.*, 1982; Aung and Worku, 1986a, b; Rao and Morris, 1967-1968; Boulama and Galanis, 2004).

In spite of its importance, only a few literature was devoted to the analysis of entropy generation due to mixed convection through channels between parallel plates. In this regard, Mahmud and Fraser (2002) gave special focus to the entropy generation characteristics and its dependency on the various dimensionless parameters during their analysis of the mixed convection-radiation interaction in a vertical channel. The results of this study showed that the optimum radiation parameters determined based on the concept of EGM, increase with $(Gr \times Ri)^{0.5}$ where Ri is the Richardson number that equals Gr/Re^2. This means that the value $(Gr \times Ri)^{0.5}$ used in Mahmud and Fraser (2002) is equivalent to the modified buoyancy parameter (Gr/Re) used in the present work. It is worth mentioning here that the non-dimensionlization procedure used in this article which led to the appearance of the parameter, Gr/Re, was used also by Aung and Worku (1986a, b), Aung (1987), Barletta (2001, 2002), Humaira Tasnim and Mahmud (2002), Mete and Orhan (2007), Boulama and Galanis (2004) and Boulama *et al.* (2006).

Boulama *et al.* (2006) investigated the steady-state, laminar, fully developed mixed convection of a binary non-reacting gas mixture flowing upwards in a vertical parallel-plate channel from the second law of thermodynamics point of view. Analytical expressions were derived for the entropy generation rate for two combinations of boundary conditions: uniform wall temperature with uniform wall concentration and uniform wall heat flux with uniform wall concentration. Cheng *et al.* (1994) have numerically predicted the entropy generation of developing laminar mixed convection flow in vertical parallel plates with a series of transverses fins placed on the hotter plate. Their study showed that although fins enhance heat transfer, they cause a significant increase in entropy generation. In their study, volumetric entropy generation profiles for different height of fins were obtained and compared with the entropy generation in smooth channels. Balaji *et al.* (2007) reported the results of their numerical investigation of turbulent mixed convection from a symmetrically heated vertical channel, bathed by a steady upward flow of cold air. In this regard, they reported that the optimal inlet velocities at which the total entropy generation rate reaches a minimum value were found to exist, for every set of heat flux and aspect ratio. Further, this optimum velocity turns out to be independent of the aspect ratio and increases linearly with the heat flux. Recently, Mokheimer and Al-Salim (2009) analytically obtained the optimum values of the modified buoyancy parameters $(Gr/Re)_{\text{optimum}}$ for which the total entropy generation due to fully developed mixed convection in vertical channels between two isothermal parallel plates assumes its minimum under different operating conditions.

It is clearly noted from the literature cited above that, there is little quantitative information available on the analysis of the operating parameters effects on the entropy generation due to laminar developing mixed convection through parallel plate vertical channels. It can be also concluded that there exists no attempt in the literature to estimate the values of the modified buoyancy parameter (Gr/Re) that would result in a minimum entropy generation due to developing mixed convection through vertical channels between parallel plates under different operating conditions. This lack of information regarding the effects of the operating parameters on the entropy generation, in general, and on the optimum values of the modified buoyancy parameter, in particular, motivated the author to conduct the present study due to its importance in optimizing the design of heat transfer equipment that work under mixed convection conditions.

2. Problem description and formulation

The present article aims at developing and solving a mathematical model that predicts the overall rate of entropy generation due to mixed convection at the entrance of vertical channels between two deferentially isothermally heated parallel plates. The main objective of developing this model is to carry out a parametric analysis on the effects of the operating parameters on the entropy generation in the entry developing region. Among the investigated parameters are the modified buoyancy parameter, Gr/Re, the dimensionless temperature ratio of the two plates, θ_T, the flow Reynolds number, Re, Eckert number, Ec, and the fluid type in terms of the Prandtl number, Pr. Moreover, the effect of the operating parameters on the values of the modified buoyancy parameter at which the entropy generation assumes its minimum, $(Gr/Re)_{\text{optimum}}$, is also investigated. In this regard, Figures 1(a) and (b) depict two-dimensional channel between two vertical parallel plates. The distance between the plates, i.e., the channel width is "b". The Cartesian coordinate system is chosen such that the z-axis is in the vertical direction that is parallel to the flow direction and the gravitational force "g" always acting downwards

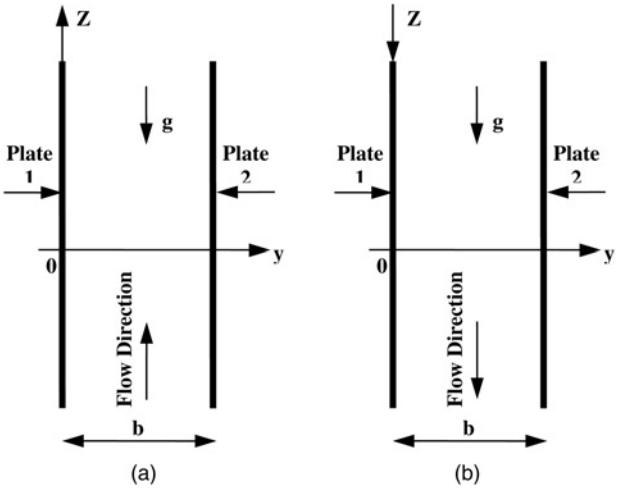

Figure 1.
Schematic view of the system and coordinate axes corresponding to (a) upflow and (b) downflow

independent of flow direction. The y-axis is orthogonal to the channel walls, and the origin of the axes is such that the positions of the channel walls are $y = 0$ and $y = b$.

The flow is assumed to be laminar and the fluid is assumed to be a Newtonian fluid with constant properties but obeys the classic Boussinesq approximation, $\rho = \rho_0(1 \mp \beta|T - T_0|)$, according to which the fluid density is treated as constant in all terms of the governing equations except in the buoyancy term of the vertical flow direction momentum equation where it is considered as a function of temperature. It is also assumed that the viscous dissipation effect on the temperature distribution is neglected while its effect on the entropy generation is considered (Yang *et al.*, 2008; Takahiro *et al.*, 2008; Ilis *et al.*, 2008; Varol *et al.*, 2008; Ordóñez and Bejan, 2000; Ko, 2006a, b, 2007a, b; Ko and Cheng, 2007; Ben Nejma *et al.*, 2008; Mahmud and Fraser, 2002; Aung, 1987; Barletta, 2001, 2002; Humaira Tasnim and Mahmud, 2002; Mete and Orhan, 2007; Boulama *et al.*, 2006; Cheng *et al.*, 1994; Balaji *et al.*, 2007; Mokheimer and Al-Salim, 2009). Considering a vertical channel between parallel plates whose depth, x-direction, is much larger than the distance between the two plates, one can reduce the problem into a two-dimensional problem. The general governing equations of flow and heat transfer are the conservation equations of mass, momentum and energy along with the entropy production equation that is used to predict the irreversibility associated with the heat and fluid flow. Assuming that the boundary layer approximation is applicable to the present problem and neglecting the axial diffusion of momentum and heat, one can convert the governing equations from elliptic into parabolic equations. This simplifies the solution while keeping the solution accuracy intact. It is worth mentioning here that the use of the parabolic boundary layer-based model has been firstly used by Bodoia and Osterle (1962) to describe the developing flow due to free convection between vertical parallel plates. Since then and till now, many researchers have used the parabolic boundary layer-based model to describe the developing forced, free and mixed convection in vertical ducts with different cross-section shapes (Schmidt and Zeldin, 1970; Feldman *et al.*, 1982a, b; Cheng *et al.*, 1995, 2000a,b; Choudhury and Patankar, 1988; Bernier and Baliga, 1992; Orfi *et al.*, 1997; Nesreddine *et al.*, 1998; Ouzzane and Galanis 2001; Cheng and Huang, 2002; Hammou *et al.*, 2004). Many of these researchers (Aung and Worku, 1986b; Feldman *et al.*, 1982b; Cheng *et al.*, 2000a, b; Cheng and Huang, 2002) have employed a two- and three-dimensional parabolic model to predict the buoyancy-assisted

flow separation and heat transfer in the entrance region of a vertical rectangular duct. Their results show that the solutions yielded by the parabolic model agree closely with the elliptic-model solutions in wide ranges of considered physical parameters. The computer memory space and computation time required in the parabolic model analysis is much less than that required in the full elliptic model. These findings clearly demonstrate the efficiency of the parabolic-model analysis. The steady-state governing equations for mixed convection between vertical parallel plates, after applying boundary layer approximation under the above listed assumptions, are:

Continuity equation:

$$\frac{\partial u}{\partial z} + \frac{\partial v}{\partial y} = 0 \tag{1}$$

z-Momentum equation

$$\rho_o \left[u\frac{\partial u}{\partial z} + v\frac{\partial u}{\partial y} \right] = -\frac{\partial (p - p_o)}{\partial z} \pm \rho_o g\beta |T - T_o| + \mu \left(\frac{\partial^2 u}{\partial y^2} \right) \tag{2}$$

where plus and minus signs indicate buoyancy aiding flow and buoyancy opposing flow, respectively.

Energy equation

$$u\frac{\partial T}{\partial z} + v\frac{\partial T}{\partial y} = \frac{k}{\rho_o C_p} \left(\frac{\partial^2 T}{\partial y^2} \right) \tag{3}$$

To complete the mathematical model in order to solve for the four unknowns, u, v, T and p, appeared in the three governing equations listed above, one more equation is required. This equation is the integral form of the continuity equation.

Integral continuity equation

$$\overline{u} = \frac{1}{b} \int_0^b u dy \tag{4}$$

Solving the above set of equations (equations (1)-(4)), one can obtain the temperature and velocity profiles at each plane downstream from the channel entrance to the fully developed region. Having the temperature and velocity profile, one can calculate the volumetric local thermal, viscous and total entropy generation at each plan of the channel. The thermal entropy generation is attributed to the heat transfer across the fluid due to temperature difference while the viscous entropy generation is attributed to the viscous dissipation associated with the flow of viscous fluids. The volumetric rate of local total entropy generation can be expressed as the sum of the volumetric rate of local thermal entropy generation and the volumetric rate of local viscous entropy generation as:

Dimensional volumetric rate of local entropy equation

$$s'''_{gen} = s'''_{Thermal} + s'''_{Viscous}$$

$$s'''_{gen} = \frac{k}{T^2}\left[\left(\frac{\partial T}{\partial z}\right)^2 + \left(\frac{\partial T}{\partial y}\right)^2 + \left(\frac{\partial T}{\partial x}\right)^2\right] + \frac{\mu}{T}\left\{2\left[\left(\frac{\partial u}{\partial z}\right)^2 + \left(\frac{\partial v}{\partial y}\right)^2 + \left(\frac{\partial w}{\partial x}\right)^2\right] + \left(\frac{\partial v}{\partial z} + \frac{\partial u}{\partial y}\right)^2 + \left(\frac{\partial w}{\partial y} + \frac{\partial v}{\partial x}\right)^2 + \left(\frac{\partial w}{\partial z} + \frac{\partial u}{\partial x}\right)^2\right\} \quad (5)$$

Obtaining the volumetric rate of local entropy generations via the direct substitution of the temperature and velocity gradients in the above equation, one can obtain the overall rate of total entropy generation by integrating the volumetric rate of local entropy generation over the volume under consideration. This integration can be expressed in the following form:

$$s_{Tot} = \int_V s'''_{gen}(y,z,x)dV = \int_0^x \int_0^l \int_0^b s'''_{gen}(y,z,x)dydzdx \quad (6)$$

Having the channel depth, in x-direction, much larger than the channel width, in y-direction and the channel height, in z-direction, the two dimensions considerations can be applied to the entropy generation equation (5) and it can be reduced to:

$$s'''_{gen} = \frac{k}{T^2}\left[\left(\frac{\partial T}{\partial z}\right)^2 + \left(\frac{\partial T}{\partial y}\right)^2\right] + \frac{\mu}{T}\left\{2\left[\left(\frac{\partial u}{\partial z}\right)^2 + \left(\frac{\partial v}{\partial y}\right)^2\right] + \left(\frac{\partial u}{\partial y} + \frac{\partial v}{\partial z}\right)^2\right\} \quad (7)$$

Moreover, the overall rate of total entropy generation given by equation (6) reduces to:

$$\frac{s_{Tot}}{w} = \int_0^l \int_0^b s'''_{gen}(y,z)dydz \quad (8a)$$

where w is the depth of the channel which is very large compared to the channel width and height. It is worth noting also that the rate of entropy generation per plan across the channel width can be obtained from the integration of the volumetric rate of local entropy generation over that plan as given by the following equation:

$$\frac{s'_{Toty}}{w} = \int_0^b s'''_{gen}(y,z)dy \quad (8b)$$

The governing equations (1)-(4) are subjected to the following hydrodynamic and thermal boundary conditions.

Entrance condition:

$$\text{At} \quad z = 0, \quad 0 < y < b: \; u = u_o, \quad v = 0, \quad p = p_{o,} \quad T = T_o \quad (9)$$

No slip conditions:

$$\text{At} \quad y = 0: \; u = v = 0, \quad \text{at} \quad y = b: \; u = v = 0 \tag{10}$$

Thermal boundary conditions:

$$\text{At} \quad y = 0: \; T = T_1, \quad \text{at} \quad y = b: \; T = T_2 \tag{11}$$

Using the dimensionless parameters given in the nomenclature, the dimensionless form of the governing equation can be written as:

Continuity equation

$$\frac{\partial U}{\partial Z} + \frac{\partial V}{\partial Y} = 0 \tag{12}$$

Z-momentum equation

$$U\frac{\partial U}{\partial Z} + V\frac{\partial U}{\partial Y} = -\frac{\partial P}{\partial Z} \pm \frac{Gr}{\mathrm{Re}}\theta + \frac{\partial^2 U}{\partial Y^2} \tag{13}$$

Energy equation

$$U\frac{\partial \theta}{\partial Z} + V\frac{\partial \theta}{\partial Y} = \frac{1}{\mathrm{Pr}}\left(\frac{\partial^2 \theta}{\partial Y^2}\right) \tag{14}$$

Integral continuity equation

$$\int_0^1 U dY = 1 \tag{15}$$

Dimensionless volumetric rate of local entropy equation

$$S_{gen} = \frac{s'''_{gen} D_h^2}{k} = \frac{1}{(\theta+\tau)^2}\left[\frac{1}{\mathrm{Re}^2}\left(\frac{\partial \theta}{\partial Z}\right)^2 + \left(\frac{\partial \theta}{\partial Y}\right)^2\right] + \frac{Ec\mathrm{Pr}}{\mathrm{Re}^2}\frac{1}{(\theta+\tau)} \times \left\{2\left[\left(\frac{\partial U}{\partial Z}\right)^2 + \left(\frac{\partial V}{\partial Y}\right)^2\right] + \left(\mathrm{Re}\frac{\partial U}{\partial Y} + \frac{1}{\mathrm{Re}}\frac{\partial V}{\partial Z}\right)^2\right\} \tag{16a}$$

or: $S_{gen} = S_{Thermal} + S_{Viscous}$, where:

$$S_{Thermal} = \frac{1}{(\theta+\tau)^2}\left[\frac{1}{\mathrm{Re}^2}\left(\frac{\partial \theta}{\partial Z}\right)^2 + \left(\frac{\partial \theta}{\partial Y}\right)^2\right] \tag{16b}$$

$$S_{Viscous} = \frac{Ec\mathrm{Pr}}{\mathrm{Re}^2}\frac{1}{(\theta+\tau)}\left\{2\left[\left(\frac{\partial U}{\partial Z}\right)^2 + \left(\frac{\partial V}{\partial Y}\right)^2\right] + \left(\mathrm{Re}\frac{\partial U}{\partial Y} + \frac{1}{\mathrm{Re}}\frac{\partial V}{\partial Z}\right)^2\right\} \tag{16c}$$

The rate of entropy generation per plan can be expressed as:

$$S_{Toty} = \int_0^1 S_{gen}(Y,Z)dY \tag{17a}$$

and the overall rate of entropy generation across the whole channel can be expressed as:

$$S_{Tot} = \mathrm{Re} \cdot \int_0^L \int_0^1 S_{gen}(Y,Z)dYdZ \tag{17b}$$

Subjected to the following dimensionless hydrodynamic and thermal boundary conditions:

Entrance conditions:

$$\text{At} \quad Z = 0,\ 0 < Y < 1:\ U = 1,\ V = P = \theta = 0 \tag{18}$$

No slip conditions:

$$\text{At} \quad Y = 0:\ U = V = 0, \quad \text{at} \quad Y = 1:\ U = V = 0 \tag{19}$$

Thermal boundary conditions:

$$\text{At} \quad y = 0:\ \theta = 1, \quad at \quad y = b:\ \theta = \theta_T \tag{20}$$

3. Numerical method of solution

In the present work, an implicit finite difference scheme is developed using the techniques explained in Carnahan *et al.* (1969) to solve the governing equations for the flow and heat transfer parameters. The independent variables in this work are Y and Z. Therefore, a two-dimensional numerical grid in the Y-Z plan is imposed on the flow field as shown in Figure 2.

Mesh points are numbered consecutively from the arbitrary origin progressing in the (Y) direction perpendicular to the flow direction (Z) with $k = 1, 2, \ldots, n+1$. In this domain $k = 1$ represents the left wall and $k = n+1$ represents the right wall. It is worth mentioning that "n" being the number of segments in the Y-direction, ΔY and ΔZ are the increments in Y-direction and Z-direction, respectively. The solution is marching in the direction of flow (Z) in the form of axial steps. Hence, the quantity for example $U(Y)$ is replaced by $U(k)$. Considering the grid network shown in Figure 2, equations (12)-(15) can be written in the following finite difference forms:

Finite difference formulation of continuity equation

$$\begin{aligned} V(k) = &\left\{ V(k+1) + \frac{\Delta Y}{2\Delta Z}[U(k+1) + U(k) - U^*(k+1) - U^*(k)] \right\} Y \\ &+ \left\{ V(k-1) - \frac{\Delta Y}{2\Delta Z}[U(k-1) + U(k) - U^*(k-1) - U^*(k)] \right\} (1-Y) \end{aligned} \tag{21}$$

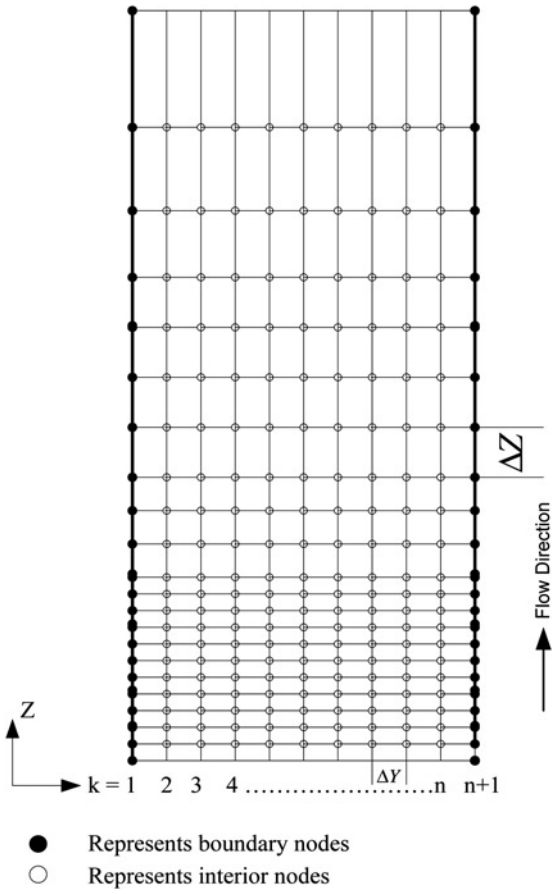

Figure 2.
Finite difference domain of a two-dimensional vertical channel between parallel plates

Finite difference formulation of the axial momentum equation:

$$-U(k)\left[U^*(k)\frac{(\Delta Y)^2}{\Delta Z}+2\right]+U(k+1)\left[1-V^*(k)\frac{\Delta Y}{2}\right]+U(k-1)\left[V^*(k)\frac{\Delta Y}{2}+1\right]$$
$$-P(k)\frac{(\Delta Y)^2}{\Delta Z}=-P^*(k)\frac{(\Delta Y)^2}{\Delta Z}-\frac{[U^*(k)\Delta Y]^2}{\Delta Z}-\left(\pm\frac{Gr}{\mathrm{Re}}\right)(\Delta Y)^2\theta(k) \quad (22)$$

Finite difference formulation of the energy equation

$$-\left[2+\mathrm{Pr}U^*(k)\frac{(\Delta Y)^2}{\Delta Z}\right]\theta(k)+\theta(k+1)\left[1-\mathrm{Pr}V^*(k)\frac{\Delta Y}{2}\right]$$
$$+\theta(k-1)\left[1+\mathrm{Pr}V^*(k)\frac{\Delta Y}{2}\right]=-\mathrm{Pr}U^*(k)\theta^*(k)\frac{(\Delta Y)^2}{\Delta Z} \quad (23)$$

where "*" represents the previous axial step value and plus and minus in the term $(\pm Gr/\mathrm{Re})$ indicates the buoyancy-aiding and buoyancy-opposing flow.

Numerical representation of the integral continuity equation

The integral continuity equation can be represented by employing a trapezoidal rule of numerical integration and is as follows.

$$\left[\sum_{k=2}^{n} U(k) + 0.5(U(1) + U(n+1))\right]\Delta Y = 1$$

However, from the no-slip boundary conditions:

$$U(1) = U(n+1) = 0$$

Therefore, the integral equation reduces to:

$$\left[\sum_{k=2}^{n} U(k)\right]\Delta Y = 1 \tag{24}$$

The method of solving the above equations (21)-(24) to get U, V, θ and P is discussed below. Once the values of U, V and θ are obtained, they are substituted in the volumetric entropy equations. The finite difference formulation of the volumetric thermal and viscous entropy generation are given as follows:

$$S_{Thermal} = \frac{1}{(\theta(k)+\tau)^2}\left[\frac{1}{\mathrm{Re}^2}\left(\frac{\theta(k)-\theta^*(k)}{\Delta Z}\right)^2 + \left(\frac{\theta(k+1)-\theta(k)}{\Delta Y}\right)^2\right] \tag{25}$$

$$S_{Viscous} = \frac{Ec\mathrm{Pr}}{\mathrm{Re}^2}\frac{1}{(\theta(k)+\tau)}\left\{2\left[\left(\frac{U(k)-U^*(k)}{\Delta Z}\right)^2 + \left(\frac{V(k+1)-V(k)}{\Delta Y}\right)^2\right] + \left(\mathrm{Re}\frac{U(k+1)-U(k)}{\Delta Y} + \frac{1}{\mathrm{Re}}\frac{V(k)-V^*(k)}{\Delta Z}\right)^2\right\} \tag{26}$$

For a fluid of a given Pr flowing with a given Re and Ec numbers, the numerical solution of the foregoing finite difference equations is obtained by first selecting a value of Gr/Re. By selecting the numbers of increments in Y, (n), the values of $\Delta Y = 1/n$ can be computed. The finite difference energy equation (23) has been linearized by taking the values of the coefficients of the convective terms (i.e. U* and V*) from the preceding axial step. For a given axial location (cross-section), equation (23) is applied at each grid point in the cross-section next to the entrance cross-section (i.e. with $i = 2, 3, \ldots, n-1, n$) taking into consideration the thermal boundary conditions. This results in $(n-1)$ simultaneous linear algebraic equations in the same number of unknowns. Solving this set of equations by any matrix technique (Gauss-Seidel iteration scheme (Carnahan *et al.*, 1969) has been used in the present work), one gets the unknown values of θ's at all points of the second cross-section. The obtained values of θ's are used in the solution of the linearized finite difference axial momentum equation (22). This equation

together with the integral continuity equation (24) represents two equations in two unknowns (U and P). Applying equation (24) throughout the second cross-section, equation (22) at each interior node of the numerical grid (i.e. with $k = 2, 3, \ldots, n-1, n$) and the boundary conditions (i.e. $U(1) = U(n+1) = 0$), one obtains $[(n-1)(n-1)+1]$ simultaneous linear equations in the same number of unknowns ($U(2)$, $U(3)$, …, $U(n)$, *and* P). Solving these equations by means of Gauss-Jordan elimination scheme (Carnahan *et al.*, 1969), one gets the unknown values of U's and P at all points of the second cross-section. Equation (21) is used to obtain the unknown values of V at all interior nodes. Obtaining all values of θ's, U's and V's, equations (25) and (26) are used to evaluate the volumetric rate of local thermal and viscous entropy generations, respectively. Adding these two components of the entropy generation, the volumetric rate of local total entropy generation is obtained as per equation 16(a). The volumetric rate of local thermal, local viscous and local total entropy generation can be integrated across the channel to obtain the rate of thermal, viscous and total entropy generation per each plan of the channel using equation 17(a). Repeating this procedure, one can advance axially downstream along the channel until full development is achieved or flow reversal that leads to flow and/or numerical instability is encountered. The overall thermal, viscous and total entropy generation in the whole flow domain can be calculated numerically by integrating the volumetric rate of local entropy generation values over a defined volume of the channel, from the channel entrance to any location Z downstream, using equation 17(b).

To reduce the effect of linearization and increase the accuracy of the numerical solution, a very small axial mesh sizes was used, particularly near the entrance, where the gradients are expected to be large. The results to be presented here have been obtained by using very small axial steps near the entrance (ΔZ of 10^{-10} for all the cases considered) then the axial step was increased gradually to a final value of $DZ = 10^{-3}$ as the flow approaches full development with almost negligible effect on the flow results. On the other hand, to ensure the numerical solution independence of the numerical grid size in the transverse, Y, direction, a numerical solution grid independent test was conducted and the value of the total entropy generation was estimated for grid sizes ranged from ten to 100 increments in the transverse direction. The variation of the numerically estimated overall rate of total entropy generation with the numerical grid size is reported in Figure 3(a). This figure shows that the overall rate of total entropy generation estimated numerically becomes independent of the grid size for a grid of about 45 increments or above. To guarantee the numerical accuracy, a grid of 50 increments was used to generate all the results reported in this article. It is worth reporting here that the use of non-uniform grid that has very small grid size near the walls and coarse grid is recommended. This would ensure the accurate predictions of the high gradients at the walls and guarantee less computational time due to the use of coarse grid size away from the wall. However, the use of non-uniform grid would make the numerical presentation of the governing equations as well as the programming a bit complicated. On the other hand, the use of uniform grid would result in a simpler numerical presentation of the governing equations as well as the programming of it to get the numerical solution. In the present work a uniform very small size grid has been used to simplify the numerical presentation and coding it and guarantee accurate prediction of the gradients at the wall. To ensure the adequacy of the present numerical scheme algorithm and computer code, the presently obtained numerical solutions were validated via comparing it with the previously reported work. In this regard, the development of the velocity and the mean, the pressure and

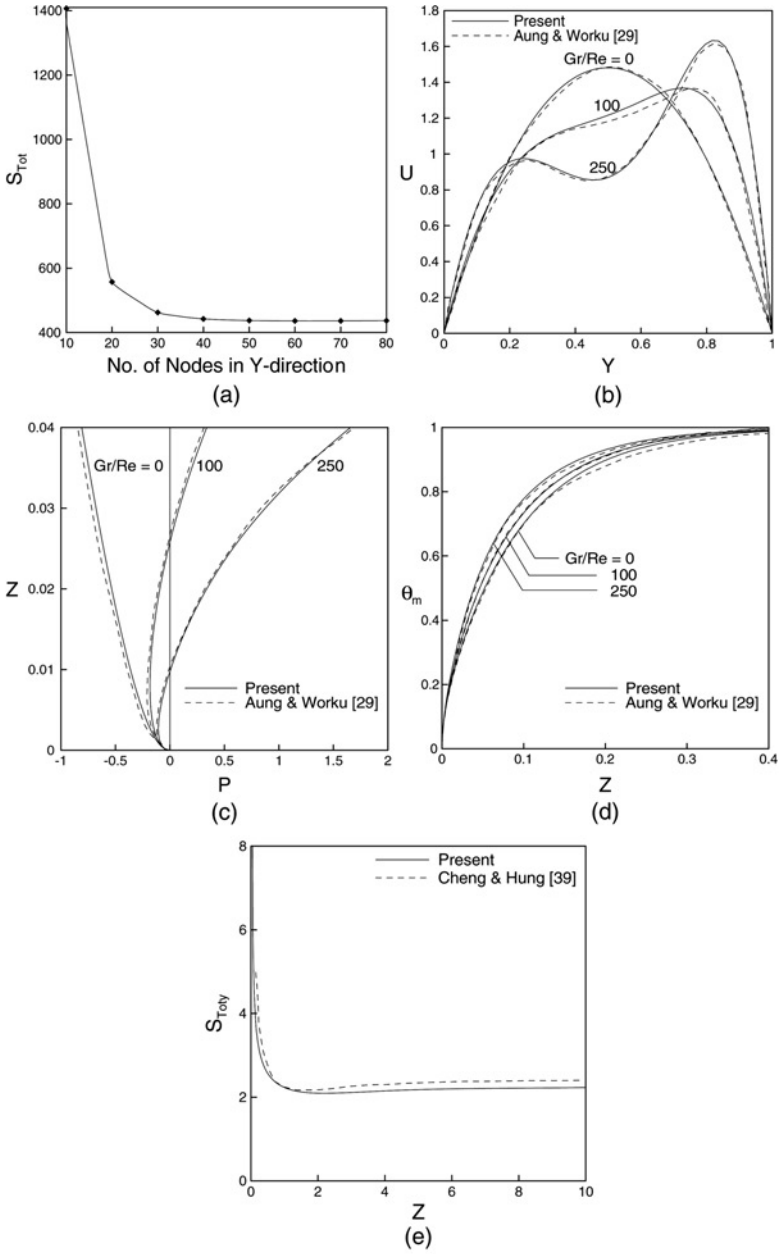

Notes: (a) Grid independent test, for $Gr/Re =$, Re = 1,000, Ec = 0.1, Pr = 0.7, $\theta_T = 0$; (b) velocity profiles for $Gr/Re = 0$, 100 and 250, $\theta_T = 0.5$ at $Z = 0.04$; (c) pressure variation for $Gr/Re = 0$, 100 and 250, $\theta_T = 1.0$ along the channel height; (d) development of mean temperature for $Gr/Re = 0$, 100 and 250 for $\theta_T = 1.0$; (e) development of rate of total entropy generation across the channel width for $Gr/Re = 125$, Re = 50, $Ec.\Pr = 0.1$, $\theta_T = 0$, $\tau = 1$

Figure 3.

mean bulk fluid temperature profiles for the two cases with the temperature ratio of the two plates $\theta_T = 0.5$ and 1 were compared to their corresponding profiles reported earlier by Aung and Worku (1986b). Figure 3(b) shows a comparison of velocity profiles between the present results and Aung and Worku (1986b) for $Gr/Re = 0$, 100 and 250 at $\theta_T = 0.5$ at an axial length of $Z = 0.04$. Figure 3(c) shows the variation of pressure at $\theta_T = 1.0$. On the other hand, Figure 3(d) shows the comparison of the development of the mean bulk fluid temperature for $\theta_T = 1.0$. Moreover, the code is also validated via comparing the development of the rate of total entropy generation per plan across the channel of the present work with the work of Cheng *et al.* (1994) as presented in Figure 3(e). All the comparisons of the results show excellent agreement with the previously published works which proves the accuracy of the numerical solution predicted presently using a uniform grid of very small size in the transverse direction as indicated above. Moreover, all the numerical results presently predicted for the fully developed region are in excellent agreement with their pertinent analytical solution as indicated in the following section. This is another strong prove of the accuracy of the presently used model numerical scheme and computer code.

4. Results presentation and discussions

Having confidence in the mathematical model, numerical scheme and the computer code via the validation briefed above, the development of temperature and velocity profiles were numerically obtained in the entrance region of the channel for a wide range of the operating parameters under consideration. These developing profiles were used to predict and analyze the development of the main heat transfer parameters (the mean bulk fluid temperature and the Nusselt number on the two walls of the channels). These profiles were also used to numerically predict the development of the volumetric rate of local thermal, viscous and total entropy generations. The development of the volumetric rate of entropy generations was used to predict the total rate of entropy generations per plan across the channel as well as the overall entropy generations throughout the whole channel from the entrance to any location Z downward under a wide range of the operating parameters.

The development of the temperature profiles for asymmetric heating/cooling ($\theta_T = 0$) and the symmetric heating/cooling ($\theta_T = 1$) for buoyancy-aided and buoyancy-opposed flows of $Gr/Re = 60$ and –60 is shown in Figures 4(a) and (b), respectively. The figures show steep temperature gradients at the entrance of the channel near the heat transfer wall for both cases of buoyancy-aided and buoyancy-opposed flows, where the maximum heat transfer rate is expected. The temperature profile will ultimately reach the fully developed linear profile downstream of the channel where the fluid flow is moving in lamina. The convective term in the energy equation vanishes, and the only term that remains in the energy equation is the transverse conduction term. Un-presented figures show the development of the axial gradient of the temperature ($d\theta/dZ$) across the channel, where it fades away upon reaching the thermally fully developed region. It also shows that the axial gradient of the temperature increases from zero at the hot/cold wall for both cases of buoyancy-aided and buoyancy-opposed flows, respectively, until it reaches a maximum, then reduces gradually back to zero at the cold/hot wall. The transverse gradient of the temperature profiles continue developing from the channel entrance non-uniformly near the channel entrance until it reaches a uniformly constant value in the fully developed region that depends on the value of the two walls temperature ratio.

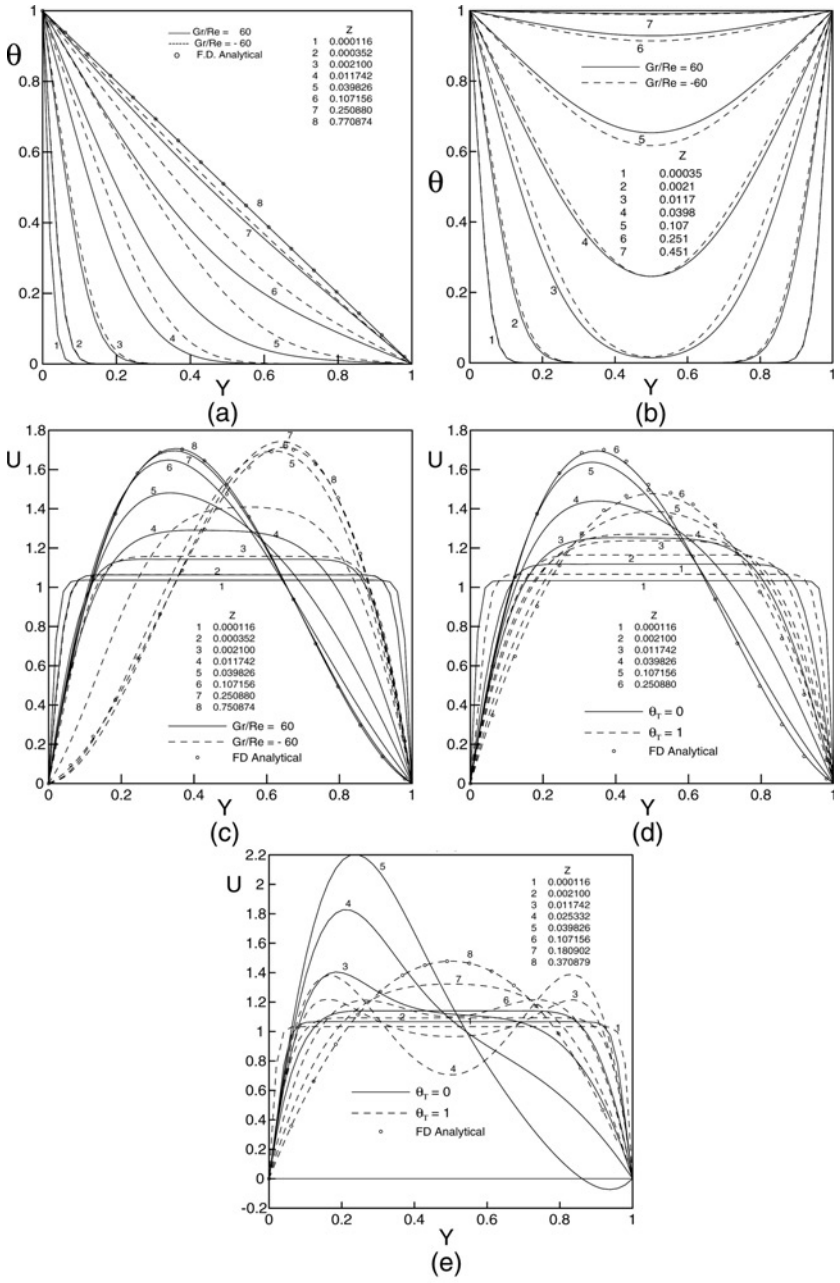

Notes: (a) Development of the temperature profiles for $Gr/Re = 60$ & -60 for $\theta_T = 0$; (b) development of the temperature profiles for $Gr/Re = 60$ & -60 for $\theta_T = 1$; (c) development of axial velocity profiles between vertical parallel plates for $Gr/Re = 60$ & -60; (d) development of axial velocity profiles for $Gr/Re = 60$ and $\theta_T = 0$ & 1; (e) development of axial velocity profiles for $Gr/Re = 250$ and $\theta_T = 0$ & 1, Pr = 0.7

Figure 4.

For example, the fully developed temperature gradient equals -1 for $\theta_T = 0$ and equals 0 for $\theta_T = 1$, as shown in Figures 4(a) and (b). It is clear that the temperature profiles develop faster for buoyancy-opposed flows compared to those for buoyancy-aided flows of the same modified buoyancy parameter. It is also clear that the gradients of the developing temperature profiles are almost the same right downstream the channel entrance, profiles 1 and 2 of Figure 4(a). Farther downstream, the developing temperature profiles for buoyancy-aided flows have higher gradients compared to those of the buoyancy-opposed flows. This behavior results in higher volumetric rate of thermal entropy generation for developing buoyancy-aided flows compared to that of the buoyancy-opposed flows. For the case of symmetric heating (or cooling), after the channel entrance the temperature profiles of the buoyancy-aided flow approaches faster its fully developed values with higher gradients compared to those of the buoyancy-opposed flows. This results in higher volumetric rate of local thermal entropy generation for buoyancy-aided flow near the channel entrance followed by a lower volumetric rate of local thermal entropy generation compared with the buoyancy-opposed flows for the case of symmetric heating (cooling). However, as the flow approaches the fully developed region the temperature profiles for buoyancy-aided and buoyancy-opposed flows become the same independent of the modified buoyancy parameter as well as the volumetric rate of thermal entropy generation. This is consistent with the analytical solution for the fully developed mixed convection under isothermal boundary conditions of first kind (Mokheimer and Al-Salim, 2009).

The development of the velocity profiles for asymmetric heating/cooling ($\theta_T = 0$) for buoyancy-aided and buoyancy-opposed flows of $Gr/Re = 60$ and -60 are shown in Figure 4(c). On the other hand, the developments of the velocity profiles for asymmetric heating/cooling ($\theta_T = 0$) and symmetric heating/cooling ($\theta_T = 1$) for the case of aiding flow with modified buoyancy parameter $Gr/Re = 60$ and 250 are shown in Figures 4(d) and (e), respectively. The presented profiles show that, for the asymmetric heating/cooling, the fluid decelerates at the two walls due to the no-slip condition and accelerates at the core to satisfy the continuity principle. Farther downstream of the channel, the fluid near the hot wall gains more heat and accelerates, shifting the peak of the profile towards the hot wall. This distortion of the velocity profile away from its parabolic profile of the pure forced flows ($Gr/Re = 0$), increases with the increase of the modified buoyancy parameter to the extent of flow reversal occurrence for a modified buoyancy parameter of ± 72 as it was obtained analytically for the asymmetric heating/cooling case of ($\theta_T = 0$) (Mokheimer and Al-Salim, 2009). The flow reversal takes place at the cold wall (plate 2 for buoyancy-aided flows and plate 1 for buoyancy-opposed flows). These highly distorted velocity profiles result in high velocity gradients at the walls and in the core of the channel as it is shown in Figures 4(c) and (e). This results in higher levels of volumetric rate of local viscous entropy generation as it is reported hereinafter for the cases of asymmetric heating. More figures that show the effects of the modified buoyancy parameter Gr/Re on the development of the velocity profiles and the resultant distorted profiles for the asymmetric heating/cooling are given in Mokheimer (2009). On the other hand, for the case of symmetric heating/cooling ($\theta_T = 1$), the fluid decelerates at the two walls due to the no-slip condition and accelerates at the core to satisfy the continuity principle. For small values of the modified buoyancy parameters, the velocity profiles for the symmetric heating/cooling ($\theta_T = 1$) develops similar to that for pure forced convection with their peaks are always in the vicinity of the channel core, as shown in Figure 4(d). However, for the symmetric heating/cooling at high values of the modified buoyancy parameters, e.g.

$Gr/Re = 250$, the velocity profiles are distorted near the entrance acquiring two peaks near the heat transfer walls with lower velocities in the channel core. Farther downstream, the heating/cooling effects of the two walls penetrate more towards the core of the channel achieving a uniformly flat temperature profile as shown in Figure 4(b) while the velocity profile approaches its parabolic shape as that of pure forced convection (isothermal flow) at the fully developed region. On the other hand, for the case of asymmetric heating/cooling for buoyancy-aided flows, the buoyancy effects highly distort the velocity profiles ($\theta_T = 0$) to the extent that it will cause flow reversal at the cold wall as shown in Figure 4(e). This trend results in lower volumetric rate of the viscous entropy generation in the channel core for the case of symmetric heating/cooling ($\theta_T = 1$) compared with the case of asymmetric heating/cooling ($\theta_T = 0$). For cases in between the symmetric and asymmetric heating/cooling (i.e. for values of $0 < \theta_T < 1$), the temperature profiles, the velocity profiles, and consequently the development of the volumetric rates of local thermal and viscous entropy generations acquire intermediate trends between the two cases reflecting the effect of the two plates temperature ratio.

The developing temperature profiles, along with the developing velocity profiles, are used to obtain the development of the mean bulk fluid temperature as described by equation (27):

$$\theta_m = \frac{\int_0^1 \theta(Y)U(Y)\,dY}{\int_0^1 U(Y)\,dY} \tag{27}$$

Equation (27) is evaluated numerically. Figure 5(a) shows the effect of the modified buoyancy parameter (Gr/Re) on the development of the mean bulk fluid temperature of the flow for the case of asymmetric heating/cooling case ($\theta_T = 0$). On the other hand, the effect of the two plates' dimensionless temperature ratio θ_T on the development of the mean bulk fluid temperature for the two cases of aiding and opposing flows with $Gr/Re = 50$ and –50, respectively, is shown in Figure 5(b). The fully developed value of the mean bulk fluid temperature has lower values for buoyancy-opposed flow and higher values for buoyancy-aided flow compared to those of pure forced convection ($Gr/Re = 0$).

The developing mean bulk fluid temperature is used to obtain the developing Nusselt number at the active and passive plates of the channel as described by equations (28a) and (28b), respectively.

$$Nu_1 = \frac{-2}{(1-\theta_m)}\left.\frac{d\theta}{dY}\right|_{Y=0} \tag{28a}$$

$$Nu_2 = \frac{2}{(\theta_T-\theta_m)}\left.\frac{d\theta}{dY}\right|_{Y=1} \tag{28b}$$

It is worth mentioning that the factor of 2 is introduced in equations (28a) and (28b) to make Nusselt number consistent with that reported in the literature (Shah and London, 1978). This is to count for the difference in the definition of the characteristic length used in the present study as the channel width that is defined presently, while it is defined as $2b$ in Shah and London (1978). Figure 5(c) depicts the development of the Nusselt number

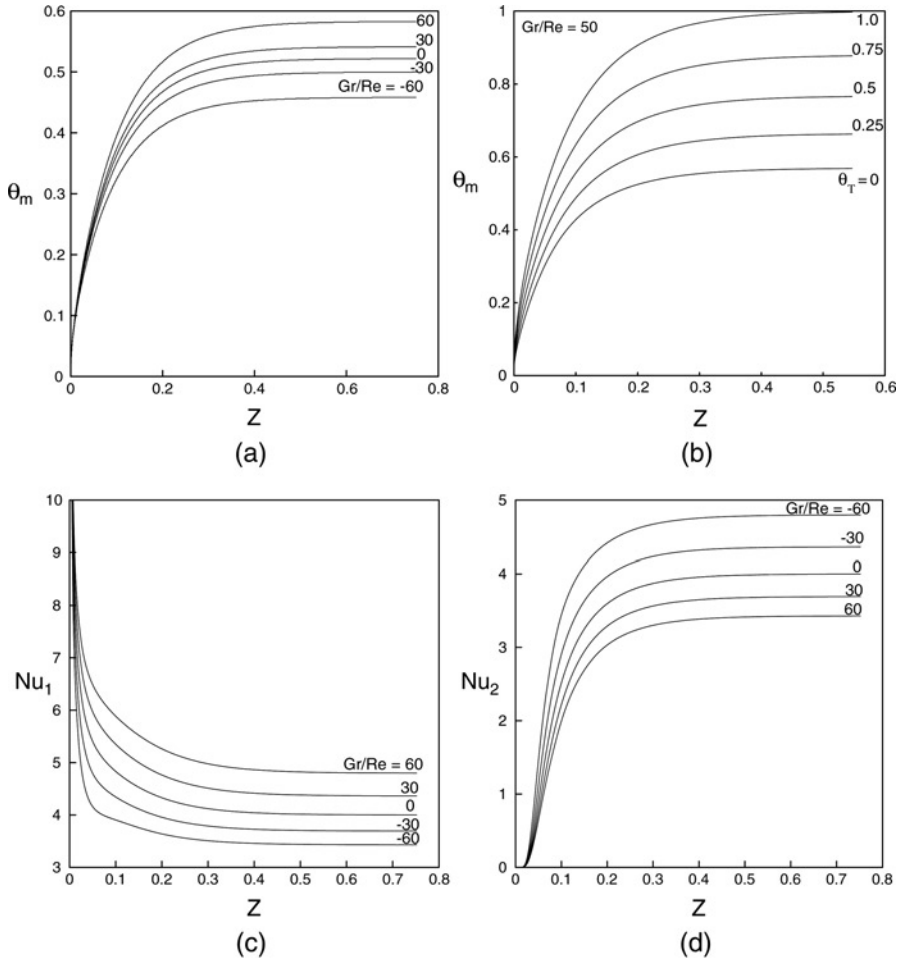

Notes: Developing of (a) mean bulk fluid temperature profiles for $\theta_T = 0$ and different Gr/Re; (b) mean bulk fluid temperature profiles for different θ_T at $Gr/Re = 50$; (c) Nusselt number at the left plate for different Gr/Re at $Pr = 0.7$; (d) Nusselt number at the right plate for different Gr/Re at $Pr = 0.7$

Figure 5.

at the hot/cold plate for the buoyancy-aided/buoyancy-opposed flows, respectively, for asymmetric heating/cooling cases. The Nusselt number on this plate of the channel develops from its high value, and then gradually decreases till it reaches its constant fully developed value far downstream of the channel. Moreover, the figure shows that the Nusselt number at the hot/cold plate for buoyancy-aided flow is higher than that for buoyancy-opposed flows. On the other hand, Figure 5(d) shows the development of the Nusselt number on the cold/hot plate of the channel for buoyancy-aided/buoyancy-opposed flows, respectively. The Nusselt number at this plate has the opposite trend to that at the other plate for asymmetric heating/cooling of the channel. The Nusselt number at this plate of the channel increases from zero till it reaches its fully developed value far downstream of the channel. Furthermore, the Nusselt number has higher values

for buoyancy-opposed flow compared to that for buoyancy-aided flow at this plate of the channel. It is worth reporting here that the values of the Nusselt number at the hot/cold and the cold/hot plates of the channel for buoyancy-aided/buoyancy-opposed flows predicted using the presently developed code as 4.001 and 3.999 as presented in Figures 5(b) and (c), respectively, compared to the value of 4 as reported in Shah and London (1978) for the case of pure forced convection ($Gr/Re = 0$) and the asymetric heating/cooling case of ($\theta_T = 0$). This represents a deviation of about 0.025 percent in both cases which is considered as another validation of the presently developed mathematical model, numerical scheme and the computer solution code. The variation of the averaged Nusselt number on hot/cold plate and the averaged Nusselt number on the cold/hot plate with the modified buoyancy parameter for different values of the dimensionless plates' temperature ratio, θ_T, is shown in Figure 5(d). The high/low heat transfer rates for the buoyancy-opposed/buoyancy-aided flows result in higher entropy generation rates. These values of Nusselt number for buoyancy-aided/buoyancy-opposed flows suggest high/low heat transfer rates that should be associated with high/low rates of thermal entropy generations.

Un-presented figures of the development of the volumetric rate of local thermal, local viscous and local total (thermal + viscous) entropy generation profiles as reported by Mokheimer (2009) for buoyancy-aided and buoyancy-opposed flows show the effect of the modified buoyancy parameter and other operating parameters on the development of the entropy generation. These volumetric rates of local thermal, viscous and total entropy generation have been integrated across the channel width using equation (17a) to predict the rate of the entropy generations per plan of the channel. The development of the rate of total (thermal + viscous) entropy generation per plan across the channel width is presented in Figures 6(a), (b) and, (c) for different values of the modified buoyancy parameter (Gr/Re), the inlet fluid dimensionless temperature (τ) and the dimensionless temperature ratio of the two plates (θ_T), respectively. These figures show that the rate of total entropy generation per plan across the channel develops from its very high value at the entrance of the channel, asymptotically, reaching its fully developed value far downstream of the channel with different gradients for different values of the operating parameters in the developing entry region. It is worth mentioning that all the values of the fully developed rate of thermal, viscous and total entropy generation per plan across the channel that have been numerically obtained via the present code (of the developing region) are in excellent agreement with their pertinent analytical fully developed solutions reported by Mokheimer and Al-Salim (2009). These excellent agreements are considered as a validation for the present model, numerical scheme and the computer code of the developing region.

The overall rate of total entropy generation across the whole channel from the entrance to any location Z downstream, given by equation (17b), can be obtained via the integration of those values given in Figures 6 (a)-(c) with respect to Z (i.e. the area under the curve in these figures). The development of the overall rate of total entropy generation for given values of Ec, Re and Pr over a wide range of the operating parameters, Gr/Re, τ and θ_T, is presented in Figures 7(a)-(c). It is worth mentioning that Figure 7(a) also depicts the overall rate of entropy generations calculated based on the assumption of fully developed conditions right from the channel entrance. The figure shows that the assumption of fully developed conditions right from the channel entrance underestimates the overall rate of entropy generation throughout the channel due to neglecting the entrance effects.

Figure 7(a) shows that the overall rate of total (thermal + viscous) entropy generation is always higher for buoyancy-opposed flows than that for buoyancy-aided

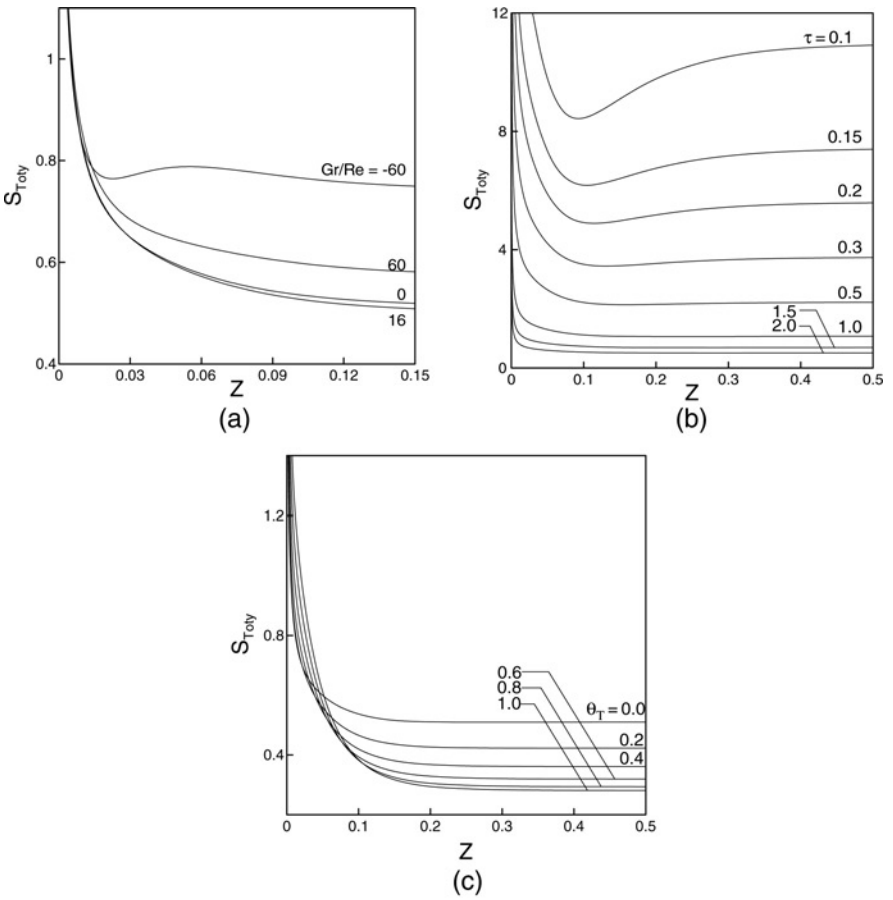

Notes: Development of the rate of (a) total thermal entropy generation; (b) viscous entropy generation; (c) total entropy generation across the channel for different Gr/Re at: $Ec = 0.1$, $\Pr = 0.7$, $\mathrm{Re} = 1{,}000$, $\tau = 2$

Figure 6.

flows. Moreover, this figure also shows that for buoyancy-aided flows, there exits an optimum value of the modified buoyancy parameter for which the overall rate of total entropy generation that counts for the entry region effects assumes its minimum below that for pure forced flow. To estimate such an optimum value of the modified buoyancy parameter $(Gr/Re)_{\mathrm{optimum}}$, the variations of the overall rate of total entropy generation with the modified buoyancy parameter Gr/Re for different values of the fluid inlet temperature ratio, τ, and for different the two plates temperature ratio, θ_T, have been plotted in Figures 8(a) and (b), respectively. Figure 8(a) shows that the overall rate of total entropy generation throughout the channel increases with the decrease of the fluid inlet temperature ratio, τ which reflects the strong entrance effects. On the other hand, Figure 8(b) shows that the overall rate of total entropy generation increases with the decrease of the two plates temperature ratio, θ_T. This explicitly reflects the effect of the increase of temperature gradients and the increase of the velocity profiles distortion with the increase of asymmetric heating/cooling. Figures 8(a) and (b) reveal that the overall rate of total

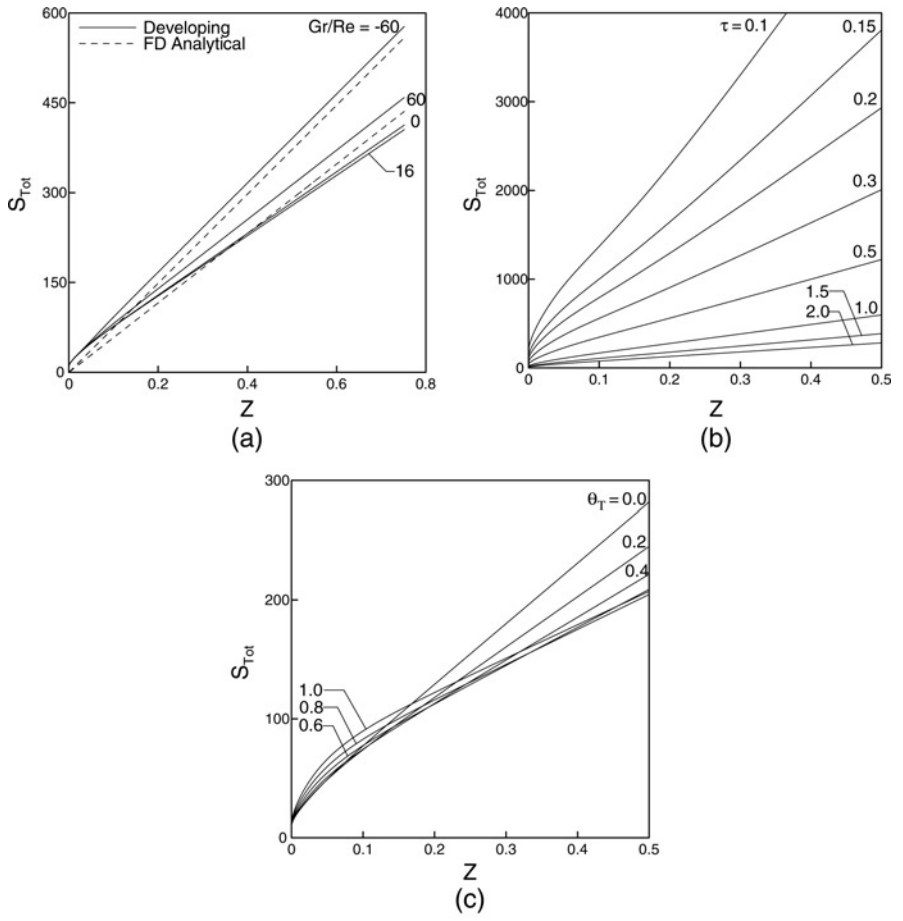

Notes: Development of the total rate of (a) thermal; (b) viscous; (c) total entropy generation rate along the channel height for different *Gr*/*Re* at: Pr = 0.7, *Ec* = 0.1, Re = 1,000, $\tau = 2$

Figure 7.

entropy generation throughout the channel has a minimal value at a certain value of the modified buoyancy parameter *Gr*/*Re*. To accurately determine these values, series of computer runs was conducted to estimate the overall rate of the thermal, viscous and total entropy generation for different values of the modified buoyancy parameter, in the vicinity of the optimum value, over a wide range of θ_T and τ for given values of *Ec*, Re and Pr. The results show the existence of one value of the modified buoyancy parameter (*Gr*/*Re*) at which minimum overall viscous entropy is generated and another value at which minimum overall total entropy is generated in the same channel under the same operating conditions. The results show also a little deviation between the two values of the modified buoyancy parameter (*Gr*/*Re*). This little deviation is attributed to the fact that the thermal entropy generation proved to be increasing with the modified buoyancy parameter in the entry developing region. A summary of the numerical obtained optimum values of the modified buoyancy parameter is given in Table I for different values of θ_T and τ for given values of Ec, Re and Pr.

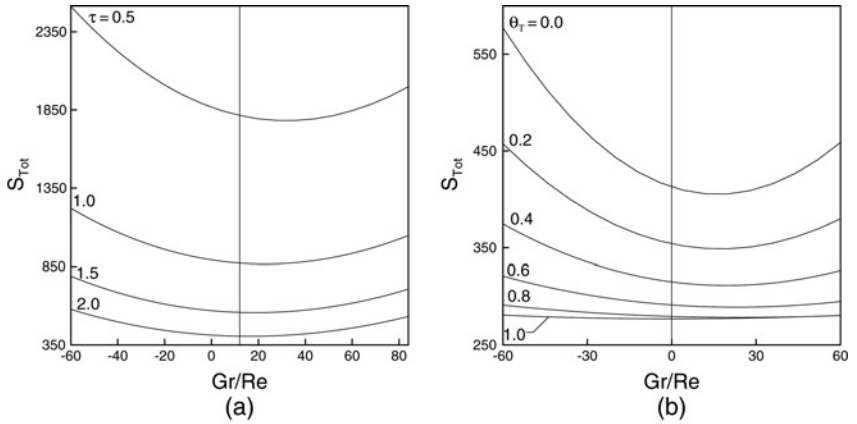

Figure 8.

Notes: Variation of the overall rate of the total entropy generation with *Gr/Re* at: Pr = 0.7; *Ec* = 0.1; Re = 1,000; *Z* = 0.752; (a) for different values of τ, $\theta_T = 0$; (b) for different values of θ_T, $\tau = 2$

The variation of the overall total entropy generation rate with *Ec* for different values of Pr is shown in Figure 9. The figure shows that the overall rate of total entropy generation varies linearly with *Ec* for all values of Pr. Another un-presented figure also shows a linear relationship between the overall rate of total entropy generation with Pr for all values of *Ec*. In other words, both *Ec* and Pr have a scaling up or scaling down effect on the overall rate of total entropy generation. It is worth mentioning that the Eckert number has no effect on the development of temperature and velocity profiles. Moreover, *Ec* has no effect on the volumetric rate of local thermal entropy generation as depicted in equation (16b). On the other hand, both *Ec* and Pr have scaling up or scalig down effect on the volumetric rate of viscous entropy generation as depicted by equation. (16c). Table II summarizes the optimum values of the modified buoyancy parameter that have been numerically obtained for different values of *Ec* for given values of θ_T, τ, *Re* and Pr. Table II gives the optimum value of the modified buoyancy parameter *Gr*/*Re* for three values of *Ec* number. The table clearly shows that there is no effect of *Ec* number on the optimum value of the modified buoyancy parameter that results in minimum viscous entropy. In fact, it is just a scaling factor for the viscous entropy. The effect it shows on the optimum value of the modified buoyancy parameter for the total entropy is only due to the comparability between the thermal and viscous entropy. The smaller the value of *Ec*, the less comparable the viscous entropy to the thermal entropy is, and *vice versa*.

The variation of the overall rate of entropy generation with the axial distance is shown in Figure 10(a) for different values of Reynolds number, Re. The figure shows that for low Reynolds number, the overall rate of total entropy generation decreases with the increase of Reynolds number. However, the overall rate of total entropy generation starts increasing again with the increase of Reynolds number. This variable behavior reveals the existence of an optimum value of Re at which the overall rate of total entropy generation assumes a minimum value. To obtain such value, the variation of the overall rate of total entropy generation with Reynolds number is depicted in Figure 10(b). The figure shows that the overall rate of total entropy generation rate decreases from a very high value at low Reynolds number which reflects high viscous effects. This decrease of the entropy generation with the increase of Re will continue till

θ_T	τ = 0.1		0.5		1		1.5		2	
	Gr/*Re* for minimum $(S_{Tot})_{Vs}$	*Gr*/*Re* for minimum S_{Tot}	*Gr*/*Re* for minimum $(S_{Tot})_{Vs}$	*Gr*/*Re* for minimum S_{Tot}	*Gr*/*Re* for minimum $(S_{Tot})_{Vs}$	*Gr*/*Re* for minimum S_{Tot}	*Gr*/*Re* for minimum $(S_{Tot})_{Vs}$	*Gr*/*Re* for minimum S_{Tot}	*Gr*/*Re* for minimum $(S_{Tot})_{Vs}$	*Gr*/*Re* for minimum S_{Tot}
0.0	58	60	33	32	24	23	20	19	17	16
0.2	48	45	32	30	24	23	21	20	18	17
0.4	44	41	33	30	26	24	23	21	21	20
0.6	45	42	35	33	29	28	26	25	24	23
0.8	48	44	37	35	31	30	28	27	26	25

Table I.
Optimum values of the modified buoyancy parameter, *Gr*/*Re* for developing flow between vertical parallel plates channel under thermal boundary conditions of first kind at different values of θ_T and τ for $Ec = 0.1$, Re = 1,000, Pr = 0.7

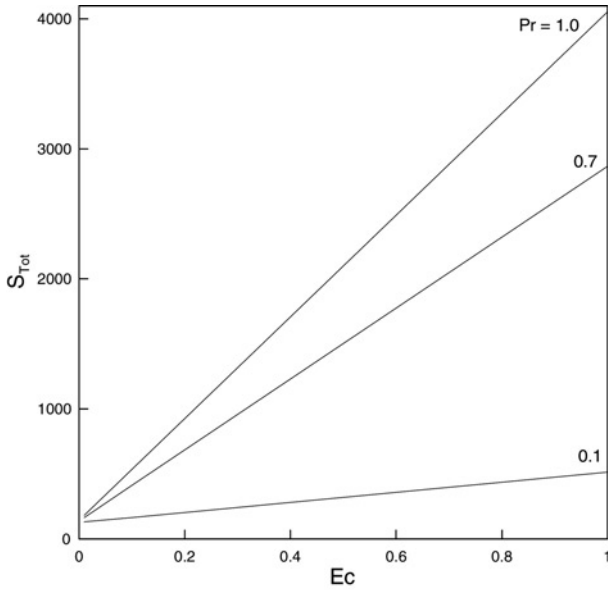

Figure 9.

Notes: Variation of overall total entropy generation rate with *Ec* for different Pr at: $Gr/Re = 30$, $Re = 1{,}000$, $\tau = 2$, $\theta_T = 0$, $Z = 0.752$

Ec					
0.01		0.1		1	
Gr/*Re* for minimum $(S_{Tot})_{Vs}$	*Gr*/*Re* for minimum S_{Tot}	*Gr*/*Re* for minimum $(S_{Tot})_{Vs}$	*Gr*/*Re* for minimum S_{Tot}	*Gr*/*Re* for minimum $(S_{Tot})_{Vs}$	*Gr*/*Re* for minimum S_{Tot}
17	9	17	16	17	17

Note: Optimum values of the modified buoyancy parameter, *Gr*/*Re*, for developing flow between vertical parallel plates channel under thermal boundary conditions of first kind at different values of *Ec* at $\theta_T = 0$, $\tau = 2$, Re = 1,000, Pr = 0.7

Table II.

it reaches a minimum value at a given Re (about 500 in the presented case) then it starts increasing with more increase in Re. This increase of the entropy generation with the increase of the Reynolds number continues as the flow moves toward turbulence.

5. Conclusions

A parametric study has been conducted on the entropy generation due to mixed convection at the entrance region of a vertical channel between isothermally and differentially heated two parallel plates. The effects of the operating parameters on the volumetric and overall rate of entropy generation have been investigated and discussed. The results revealed the existence of optimum values of the modified buoyancy parameter *Gr*/*Re* at which the total entropy generation assumes its minimum value. These values have been obtained numerically for different values of the operating

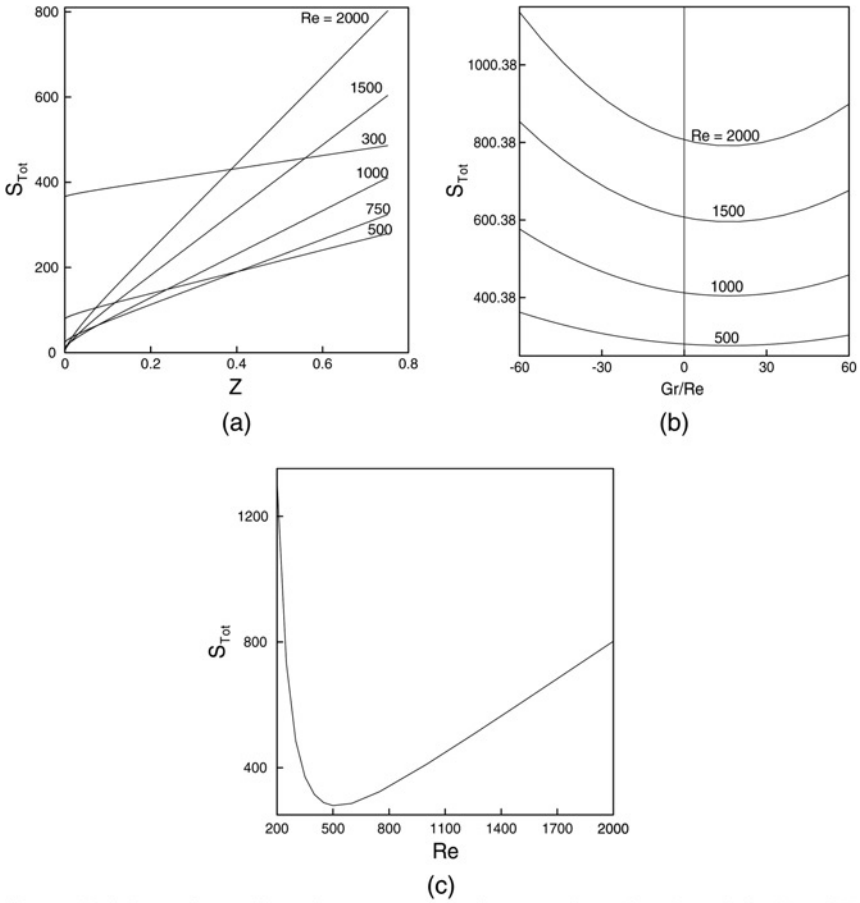

Notes: Variation of overall total entropy generation rate along the channel for Pr = 0.7, $Ec = 0.1$, $\tau = 2$, $\theta_T = 0$; (a) with Z for different *Re Gr*/*Re* = 30; (b) with *Gr*/*Re* for different Re at Z = 0.751874; (c) with Re for *Gr*/*Re* = 30, at Z = 0.752

Figure 10.

parameters. The results also revealed the existence of an optimum value of Reynolds number at which the overall rate of entropy generation assumes a minimum value under a given set of operating parameters. The effects of Eckert and Prandtl number on the entropy generation have been also investigated, presented and discussed.

References

Aung, W. (1987), "Mixed convection in internal flow", in Kakaç, S., Shah, R.K. and Aung, W. (Eds), *Hand Book of Single-Phase Convective Heat Transfer*, John Wiley & Sons, New York, NY, Chapter 15, pp. 15-1: 15-51.

Aung, W. and Worku, G. (1986a), "Theory of fully developed combined convection including flow reversal", *Journal of Heat Transfer*, Vol. 108, pp. 485-8.

Aung, W. and Worku, G. (1986b), "Developing flow and flow reversal in a vertical channel with asymmetric wall temperatures", *Transactions of the ASME, Journal of Heat Transfer*, Vol. 108, pp. 299-307.

Balaji, C., Hölling, M. and Herwig, H. (2007), "Entropy generation minimization in turbulent mixed convection flows", *International Communications in Heat and Mass Transfer*, Vol. 34, pp. 544-52.

Barletta, A. (2001), "Flow reversal of laminar mixed convection in vertical rectangular duct with one or more isothermal walls", *International Journal of Heat and Mass Transfer*, Vol. 44, pp. 3481-97.

Barletta, A. (2002), "Fully developed mixed convection and flow reversal in a vertical rectangular duct with uniform wall heat flux", *International Journal of Heat and Mass Transfer*, Vol. 45, pp. 641-54.

Ben Nejma, F., Mazgar, A., Abdallah, N. and Charrada, K. (2008), "Entropy generation through combined non-grey gas radiation and forced convection between two parallel plates", *Energy*, Vol. 33 No. 7, pp. 1169-78.

Bernier, M.A. and Baliga, B.R. (1992), "Conjugate conduction and laminar mixed convection in vertical pipes for upward flow and uniform wall heat flux", *Numerical Heat Transfer, Part A*, Vol. 21, pp. 313-32.

Bodoia, J.R. and Osterle, J.F. (1962), "The development of free convection between heated vertical plates", *Journal of Heat Transfer*, Vol. 84, pp. 40-4.

Boulama, K. and Galanis, N. (2004), "Analytical solution for fully developed mixed convection between parallel vertical plates with heat and mass transfer", *ASME Transactions, Journal of Heat Transfer*, Vol. 126, pp. 381-8.

Boulama, K.G., Galanis, N. and Orfi, J. (2006), "Entropy generation in a binary gas mixture in the presence of thermal and solutal mixed convection", *International Journal of Thermal Sciences*, Vol. 45, pp. 51-9.

Carnahan, B., Luther, H.A. and Wilkes, J.D. (1969), *Applied Numerical Methods*, Wiley, New York, NY, pp. 298-301, 450.

Cebeci, T., Khattab, A.A. and LaMont, R. (1982), "Combined natural and forced convection in vertical ducts", *Heat Transfer*, Vol. 2, pp. 419-24.

Cheng, C., Ma, W. and Hung, W. (1994), "Numerical prediction of entropy generation for mixed convective flow in a vertical channel with transverse fin array", *International Communications in Heat and Mass Transfer*, Vol. 21, pp. 519-30.

Cheng, C.-H. and Huang, S.-Y. (2002), "Predictions of mixed convection and flow reversal in a vertical duct with arbitrary cross-sectional shape", *Numerical Heat Transfer. Part A, Applications*, Vol. 41 No. 5, pp. 491-514.

Cheng, C.H., Lin, C.Y. and Aung, W. (2000a), "Predictions of developing flow with buoyancy-assisted flow separation in a vertical rectangular duct: parabolic model versus elliptic model", *Numerical Heat Transfer*, Part A, Vol. 37, pp. 567-86.

Cheng, C.H., Weng, C.J. and Aung, W. (1995), "Buoyancy effect on the flow reversal of three-dimensional developing flow in a vertical rectangular duct – a parabolic model solution", *Journal of Heat Transfer*, Vol. 117, pp. 238-41.

Cheng, C.H., Weng, C.J. and Aung, W. (2000b), "Buoyancy-Assisted Flow-Reversal and Convective Heat Transfer in Entrance Region of a Vertical Rectangular Duct", *International Journal of Heat and Fluid Flow*, Vol. 21, pp. 403-11.

Choudhury, D. and Patankar, S.V. (1988), "Combined forced and free laminar convection in the entrance region of an inclined isothermal tube", *ASME Journal of Heat Transfer*, Vol. 110, pp. 901-9.

Du Toit, C.G. (2000), "Segregated finite element solution for non-isothermal flow", *Computer Methods in Applied Mechanics and Engineering*, Vol. 182 Nos 3/4, pp. 457-81.

EPP staff report (1981), "Considerations in device cooling", *Electronic Package, Production*, Vol. 21, pp. 304-11.

Famouri, M. and Hooman, K. (2008), "Entropy generation for natural convection by heated partitions in a cavity", *International Communications in Heat and Mass Transfer*, Vol. 35 No. 4, pp. 492-502.

Feldman, E.E., Hornbeck, R.W. and Osterle, J.F. (1982a), "A numerical solution of laminar developing flow in eccentric annular ducts", *International Journal of Heat and Mass Transfer*, Vol. 25, pp. 231-41.

Feldman, E.E., Hornbeck, R.W. and Osterle, J.F. (1982b), "A numerical solution of developing temperature for laminar developing flow in eccentric annular ducts", *International Journal of Heat and Mass Transfer*, Vol. 25, pp. 243-53.

Hammou, Z.A., Benhamou, B., Galanis, N. and Orfi, J. (2004), "Laminar mixed convection of humid air in a vertical channel with evaporation or condensation at the wall", *International Journal of Thermal Sciences*, Vol. 43, pp. 531-9.

Hao, C.C. and Chung, J.N. (1995), "Direct numerical simulation of transition in mixed convection flows between two heated parallel plates", *International Journal of Numerical Methods for Heat and Fluid Flow*, Vol. 5 No. 5, pp. 399-422.

Hooman, K., Ejlali, A. and Hooman, F. (2008a), "Entropy generation analysis of thermally developing forced convection in fluid-saturated porous medium", *Applied Mathematics and Mechanics*, Vol. 29 No. 2, pp. 229-37.

Hooman, K., Gurgenci, H. and Merrikh, A.A. (2007), "Heat transfer and entropy generation optimization of forced convection in porous-saturated ducts of rectangular cross-section", *International Journal of Heat and Mass Transfer*, Vol. 50 Nos 11/12, pp. 2051-9.

Hooman, K., Hooman, F. and Mohebpour, S.R. (2008b), "Entropy generation for forced convection in a porous channel with isoflux or isothermal walls", *International Journal of Exergy (IJEX)*, Vol. 5 No. 1, pp. 78-96.

Humaira Tasnim, S. and Mahmud, S. (2002), "Mixed convection and entropy generation in a vertical annular space", *Exergy, An International Journal*, Vol. 2, pp. 373-9.

Ilis, G.G., Mobedi, M. and Sunden, B. (2008), "Effect of aspect ratio on entropy generation in a rectangular cavity with differentially heated vertical walls", *International Communications in Heat and Mass Transfer*, Vol. 35 No. 6, pp. 696-703.

Inagaki, T. and Komori, K. (1995), "Numerical modeling on turbulent transport with combined forced and natural convection between two vertical parallel plates", *Numerical Heat Transfer, Part A*, Vol. 27 No. 4, pp. 417-31.

Ko, T.-H. (2006a), "A numerical study on entropy generation and optimization for laminar forced convection in a rectangular curved duct with longitudinal ribs", *International Journal of Thermal Sciences*, Vol. 45 No. 11, pp. 1113-25.

Ko, T.H. (2006b), "Analysis of optimal Reynolds number for developing laminar forced convection in double sine ducts based on entropy generation minimization principle", *Energy Conversion and Management*, Vol. 47 No. 6, pp. 655-70.

Ko, T.H. (2007a), "A numerical study on developing laminar forced convection and entropy generation in half- and double-sine ducts", *International Journal of Thermal Sciences*, Vol. 46 No. 12, pp. 1275-84.

Ko, T.-H. (2007b), "Effects of corrugation angle on developing laminar forced convection and entropy generation in a wavy channel", *Heat and Mass Transfer*, Vol. 44 No. 2, pp. 261-71.

Ko, T.H. and Cheng, C.S. (2007), "Numerical investigation on developing laminar forced convection and entropy generation in a wavy channel", *International Communications in Heat and Mass Transfer*, Vol. 34 No. 8, pp. 924-33.

Lietzke, A.F. (1954), "Theoretical and experimental investigation of heat transfer by laminar natural convection between parallel plates", *NACA Reports*, Vol. 1223, pp. 399-405.

Mahmud, S. and Fraser, R.A. (2002), "Analysis of mixed convection – radiation interaction in a vertical channel: entropy generation", *Exergy, An International Journal*, Vol. 2, pp. 330-9.

Mete, A. and Orhan, A. (2007), "Mixed convection in a vertical parallel plate microchannel with asymmetric wall heat fluxes", *ASME Journal of Heat Transfer*, Vol. 129 No. 8, p. 1091.

Mokheimer, E.M.A. (2009), *Entropy Generation Due to Mixed Convection in Vertical Channels*, 2nd progress report, Project No. SB080006, KFUPM, March.

Mokheimer, E.M.A. and Al-Salim, A.H. (2009), "Entropy generation due to mixed convection between vertical parallel plates under isothermal boundary conditions", *International Journal of Exergy*, Vol. 6 No. 9, pp. 671-97.

Nesreddine, H., Galanis, N. and Nguyen, C.T. (1998), "Effects of axial diffusion on laminar heat transfer with low Peclet numbers in the entrance region of thin vertical tubes", *Numerical Heat Transfer, Part A*, Vol. 33, pp. 247-66.

Ordóñez, J.C. and Bejan, A. (2000), "Entropy generation minimization in parallel-plates counter flow heat exchangers", *International Journal of Energy Research*, Vol. 24, pp. 843-64.

Orfi, J., Galanis, N. and Nguyen, C.T. (1997), "Developpement simultane hydrodynamique et thermique d'un ecoulement laminaire dans un tube incline en regime de convection mixte", *Revue Generale de Thermique*, Vol. 36, pp. 83-92.

Ostrach, S. (1954), "Combined natural and forced-convection laminar flow heat transfer of fluids with and without heat sources in channels with linearly varying wall temperatures", *NACA Technical Note*, Vol. 3141, pp. 1-27.

Otani, S. and Tanaka, O. (1975), "High power semi conductor rectifier equipment using boiling and condensing heat transfer", *10th Proceedings of the IAS Conference*, pp. 46-52.

Ouzzane, M. and Galanis, N. (2001), "Numerical analysis of mixed convection in inclined tubes with external longitudinal fins", *Solar Energy*, Vol. 71 No. 3, pp. 199-211.

Peterson, G.P. and Ortega, A. (1990), "Thermal control of electronic equipment and devices", *Advances in Heat Transfer*, Vol. 20, Academic Press, San Diego, CA, pp. 181-314.

Rao, T.L.S. and Morris, W.D. (1967-1968), "Superimposed laminar forced and free convection between verical parallel plates when one plate is uniformly heated and the other is thermally insulated", *Proceedings of the Institution of Mechanical Engineers*, Vol. 182 No. 3H, pp. 374-81.

Schmidt, F.W. and Zeldin, B. (1970), "Laminar heat transfer in the entrance region of ducts", *Applied Scientific Research*, Vol. 23, pp. 73-94.

Schwiebert, M.K. and Leong, W.H. (1995), "Underfill flow as viscous flow between parallel plates driven by capillary action", *Proceedings of the 17th IEEE/CPMT International Electronic Manufacturing Technology Symposium, Austin, TX*, pp. 8-13.

Shah, R.K. and London, A.L. (1978), "Laminar flow forced convection in ducts", in Irvine, T.F. Jr and Hartnett, J.P. (Eds), *Advances in Heat Transfer, Supplement 1*, Academic Press, New York, NY.

Spiga, M. and Morini, G.L. (1996), "Laminar heat transfer between parallel plates as limiting solution for rectangular duct", *International Communications in Heat and Mass Transfer*, Vol. 23 No. 4, pp. 555-62.

Takahiro, F., Wen-Jei, Y. and Shuichi, T. (2008), "Stacked packaging laminar-convection-cooled printed circuit using the entropy generation minimization method", *Journal of Thermophysics and Heat Transfer*, Vol. 22 No. 2, pp. 315-18.

Varol, Y., Oztop, H.F. and Koca, A. (2008), "Entropy generation due to conjugate natural convection in enclosures bounded by vertical solid walls with different thicknesses", *International Communications in Heat and Mass Transfer*, Vol. 35 No. 5, pp. 648-56.

Yang, W.-J., Furukawa, T. and Torii, S. (2008), "Optimal package design of stacks of convection-cooled printed circuit boards using entropy generation minimization method", *International Journal of Heat and Mass Transfer*, Vol. 51 Nos 15/16, pp. 4038-46.

Zahmatkesh, I. (2008), "On the importance of thermal boundary conditions in heat transfer and entropy generation for natural convection inside a porous enclosure", *International Journal of Thermal Sciences*, Vol. 47 No. 3, pp. 339-46.

About the author

Esmail M.A. Mokheimer is an Associate Professor at the ME Department, KFUPM, Dhahran, Saudi Arabia, and he is on leave from Ain Shams University (ASU), Cairo, Egypt. He has published more than 40 papers in reputable international journals and conferences such as *ASME Journal of Heat Transfer, ASME Journal of Fluid Engineering, International Journal of Heat and Mass Transfer, International Journal of Numerical Methods of Heat and Fluid Flow, and Numerical Heat Transfer*. He has offered consulting services to a number of major companies in Saudi Arabia. Esmail M.A. Mokheimer can be contacted at: esmailm@kfupm.edu.sa